

BI-DIRECTIONAL REFLECTANCE DISTRIBUTION FUNCTION (BRDF) RETRIEVALS FROM LABORATORY MULTIANGLE MEASUREMENTS

Alessandro Barducci*, Donatella Guzzi, Paolo Marcoionni, Ivan Pippi

*National Research Council – Institute for Applied Physics “Nello Carrara”, via Panciatichi 64, 50127 FIRENZE, ITALY - I.Pippi@ifac.cnr.it

Submit to: “TS ThS 2 Multi-angular Sensors”

KEYWORDS: Bi-Directional Reflectance Distribution Function, multiangle observation, hyperspectral instrument, data processing, parameter retrievals.

ABSTRACT:

Theoretical investigations and intense experimental activity have been devoted to study the geometrical properties of reflection from a surface, that is expressed in terms of Bi-Directional Reflectance Distribution Function, a quantity that is relevant to many remote sensing applications, such as atmospheric modelling and climatologic studies. A large amount of laboratory and in-field measurements are now available from various systems such as the European Goniometer Facility of the Joint Research Centre, the Field Goniometer System of the University of Zurich, and the Portable Apparatus for Rapid Acquisition of Bidirectional Observation of Land and Atmosphere instrument of NASA – GSFC. Moreover, recent satellite missions such as the Multi-angle Imaging SpectroRadiometer and the Compact High Resolution Imaging Spectrometer on board of EOS-AM1 and PROBA platforms supply experimental data to this research. Following this general trend aimed to improve the current understanding of directional properties of reflection from a surface, we present laboratory multiangular observations of natural sands. These data are used in conjunction of literature data to study the reflectance dependence on surface optical and mechanical properties, illumination and viewing geometry. A simple empirical model is developed in order to retrieve Bi-Directional Reflectance Factor from experimental data. Finally, the possibility to extend the proposed physical model even to remotely sensed data is discussed, with particular reference to images gathered with CHRIS spectrometer.

1. INTRODUCTION

The knowledge of absorption of solar radiation by canopy and soil is of great interest to atmospheric modellers and climatologists, since it determines to a large extent the amount of solar energy effectively available for the whole climate system (Reichman, 1973). This absorption of radiative energy is also of concern to agronomists and biologists because it directly affects the physiology and productivity of plants (Chappelle et al, 1992).

While the amount of radiation actually absorbed by a natural target is difficult to measure, it is more practical to retrieve the absorption coefficient as a residual from the measurement of the surface and volume scattered radiation.

However, many natural surfaces exhibit preferential directions for the reflection of solar irradiance. The measured reflectance of such a surface depends not only on its structure and the position of illumination source but also on the relative position of the observer. This is the major inconvenience to estimate “conical-hemispherical” reflectance (albedo) $a(\lambda, \vartheta_0, \phi_0)$ of the surface, since the scattered radiation has to be measured over different viewing directions (Pinty and Ramond, 1986):

$$a(\lambda, \vartheta_0, \phi_0) = \frac{\int L_s(\lambda, \vartheta_0, \phi_0, \vartheta_v, \phi_v) \cos \vartheta_v d\Omega_v}{\int_{\Omega_i} L_i(\lambda, \vartheta_i, \phi_i) \cos \vartheta_i d\Omega_i} \quad (1)$$

where the denominator indicates the total irradiance impinging on the concerned target at angle (ϑ_0, ϕ_0) , $L_s(\lambda, \vartheta_0, \phi_0, \vartheta_v, \phi_v)$ the reflected radiance collected by the sensor in the direction (ϑ_v, ϕ_v) .

Spectral reflectance is generally retrieved considering the observed target as a Lambertian and homogeneous diffuser for which the upward radiance can explicitly be expressed as a function of surface reflectance (Barducci and Pippi, 1994; Qiu, 2001).

Although many surfaces behave similarly to an ideal diffuser, the above assumption will fail in two areas. The first obvious failure is that many flat surfaces have a not negligible specular component (for instance oceanic water in the visible spectral range and high-reflecting soil), i.e. an increase in the observed reflectance when the illumination and viewing zenith angles are the same and the relative azimuth angle is 180° . Many rough surfaces (like vegetation canopies) also show a reflectance increase in the “hot spot” direction when the illumination and viewing zenith angles are the same but the relative azimuth angle is null. Moreover, the error resulting from assuming Lambertian reflection for a natural target can be large for off-nadir views in remote sensing observations (Martonchik et al., 1998; Miesch et al., 2002.).

Theoretical investigations have been devoted to study the geometrical properties of reflection from a surface, that is expressed in terms of its Bi-Directional Reflectance Distribution Function (BRDF), a quantity that takes into account both the illumination and viewing geometry. The BRDF is a theoretical concept that describes the directional reflectance by relating the incident irradiance from a given direction to its contribution to the reflected radiance in another specific direction.

Intense laboratory and in-field experimental activity have also been carried out in many research institutes for better characterizing BRDF properties of natural targets. Let us remind the European GOniometric Facility (EGO) of the Joint Research Centre (at Ispra, Italy) (Sandmeier et al., 1998), the Labor-GOniometer System (LAGOS) and Field-GOniometer System (FIGOS) of the University of Zurich (Sandmeier et al., 1999), the Portable Apparatus for Rapid Acquisition of Bidirectional Observation of Land and Atmosphere (PARABOLA) instrument of NASA – GSFC (Deering and Leone, 1986), and an instrument developed at Miami University (Florida, USA), which is able to perform simultaneously multiple viewing-angle measurements (Voss et al., 2000).

Recent satellite sensors such as the Multi-angle Imaging SpectroRadiometer (MISR) on the Earth Observation Science (EOS) Terra platform (Diner et al., 1998) and the Compact High Resolution Imaging Spectrometer (CHRIS) on board of European Space Agency (ESA) Proba platform (Cutter et al., 2003) supply experimenters with their off-nadir tilting capability.

Following this general trend aimed to improve the current understanding of directional properties of reflection from a surface, we show laboratory multiangular observations of natural sands obtained with a custom instrument whose main properties are presented in Section two. Section three describes the calibration procedure to take into account the BRDF properties of reflection from a surface as measured by our instrument. Some preliminary results are presented in Section four and open problems and conclusion are drawn in Section five.

2. SYSTEM CONCEPT

Although the BRDF is an important parameter for describing the surface reflectance, its measurement is hindered even for simple surfaces from the impossibility of yielding field-of-view (FOV) having a vanishing width.

Moreover, because this function varies versus both illumination and viewing angle, many measurements are required. Therefore we have developed a suitable goniometric head for the ZEISS MCS 501 fiber optics spectrometer, whose characteristics are listed in Table I.

| | |
|----------------------|--|
| Optical entry: | Two 600 μm (core diameter) fibers with NA~0.25 for illuminating and viewing |
| Dispersing element: | Holographic concave grating with 157 grooves/mm |
| Detector array: | Hamamatsu with 1024 elements |
| Spectral range: | 215 nm – 1015 nm (nominal) 280 nm – 900 nm (working) |
| Spectral resolution: | 2-3 nm |
| Illuminating source: | Internal 75W Xenon lamp (CLX 500) |
| Digitalization: | 16 bit |

Table I. Spectral and radiometric properties of the ZEISS MCS 501 spectrometer utilised for laboratory reflectance measurements

Each fiber, which is employed for illuminating the surface and collecting the reflected radiance, is terminated with GRIN-rod lenses SLW30 to collimate the outgoing and incoming beams.

In the actual configuration the illuminating and reflected beams have a divergence of 108 mrad and a spot size diameter (at the end of the GRIN-rod) equals to 1.5 mm. Figure 1 shows a picture of the optical head employed to carry out BRDF measurements.

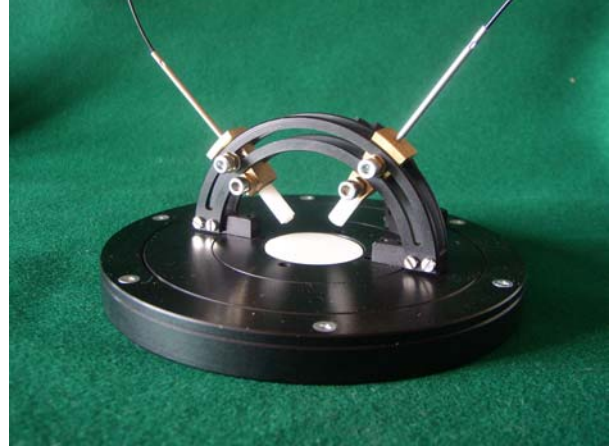


Figure 1. Picture of the optical head employed for laboratory BRDF measurements

The optical fibers are arranged on a goniometric mounting so that the centre of the illuminated spot remains fixed on the sample surface while moving the source fiber at a different illumination angle. The only change of the illuminated surface is connected with the deformation of the source spot, which becomes elliptical with increasing the viewing/illumination angle.

We have performed measurements for illumination (zenith) angles of 0° , 15° , 30° and 45° , mapping the bi-conical reflectance for different viewing angles in the source principal plane. Due to mechanical constraints position of illuminating and viewing fibers have been limited to zenith angles not greater than 60° .

3. CALIBRATION PROCEDURE

The geometrical properties of a reflecting surface are readily described by its BRDF, denoted symbolically as $\rho_{BRDF}(\lambda, \vartheta_0, \phi_0, \vartheta_r, \phi_r)$, which is defined (Nicodemus et al., 1977) as the ratio of the radiance $dL^{out}(\lambda, \vartheta_0, \phi_0, \vartheta_r, \phi_r; E_i)$ scattered into the direction (ϑ_r, ϕ_r) to the irradiance $dE_i(\lambda, \vartheta_0, \phi_0)$ impinging at angle (ϑ_0, ϕ_0) on a unitary surface area (see Figure 2 for a coordinate description):

$$\rho_{BRDF}(\lambda, \vartheta_0, \phi_0, \vartheta_r, \phi_r) = \frac{dL^{out}(\lambda, \vartheta_0, \phi_0, \vartheta_r, \phi_r; E_i)}{dE_i(\lambda, \vartheta_0, \phi_0)} \quad (2)$$

Due to its definition BRDF is a density of reflectance [sr^{-1}] and it can take values from zero to infinity. Let us note that the BRDF, defined as ratio of infinitesimals (vanishing quantities), is a derivative with instantaneous values that can not be directly

measured, since real measurements involve finite extension intervals (resolution) of the concerned geometrical parameters.

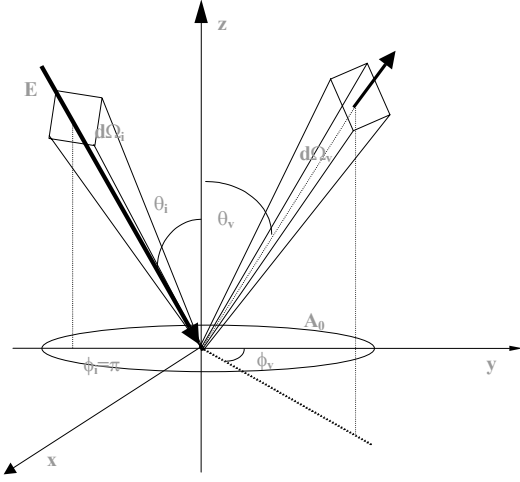


Figure 2. Diagram of the measurement geometry for BRDF. The origin of the coordinate system is the point at which the central ray of the collimated irradiance E strikes the sample surface at angle (ϑ_i, ϕ_i) with $\phi_i = \pi$. The z axis is normal to the sample surface, and the y axis lies in the plane defined by z and E . The viewing direction is given by (ϑ_v, ϕ_v) and $d\Omega_v$ is the solid angle subtended by the receiver.

A common simplification of the BRDF is to assume the concerned reflector as a Lambertian (perfectly diffuser) surface, i.e. an infinite ideal surface for which the reflected radiance is isotropic with the same value for all directions (ϑ_v, ϕ_v) regardless of how it is irradiated. Therefore, Lambertian surfaces constitute a restricted ensemble of reflectors, which are included in the more general class of natural surfaces. However, it is possible to define another class of reflectors whose bi-directional reflectance distribution function $\rho_{BRDF}(\lambda, \vartheta_i, \phi_i, \vartheta_v, \phi_v)$ is assumed to be a separable function $\rho_{BRDF}(\lambda, \vartheta_i, \phi_i, \vartheta_v, \phi_v) \approx \rho_0(\lambda)h(\vartheta_i, \phi_i, \vartheta_v, \phi_v)$. If we impose according to the definition of reflected irradiance that:

$$\int_{2\pi_v} h(\vartheta_i, \phi_i, \vartheta_v, \phi_v) \cos \vartheta_v d\Omega_v = \pi \quad (3)$$

then, we obtain an additional definition of albedo $\rho_0(\lambda)$:

$$\rho_0(\lambda) = \frac{\int_{2\pi_v} \rho_{BRDF}(\lambda, \vartheta_i, \phi_i, \vartheta_v, \phi_v) \cos \vartheta_v d\Omega_v}{\pi} \quad (4)$$

A relevant trouble to execute BRDF measurements is the necessity to perform a reference measurement over a white standard, for instance a sample of Barium Sulphate or a Spectralon tile, for any used illumination and viewing geometry. The standard experimental procedure would produce a wrong

result since the angular behavior of the investigated sample should be normalized to that of the employed reference, which has its own angular dependence.

In order to avoid mixing of angular properties of reference and target, the reference measurement has always been executed with the same geometry, namely $\vartheta_i = 0^\circ$ (indicated as $\hat{\vartheta}_0$) for the illumination angle and $\vartheta_v = 45^\circ$ (indicated as $\hat{\vartheta}_r$) for the viewing angle, in the hypothesis to get the spectral measurements in the principal plane, i.e. $\hat{\phi}_0 - \hat{\phi}_r = 180^\circ$. Utilising a collimated radiation source emitting the directional radiance $L_0(\lambda)$, it is easy to demonstrate that the flux $\Phi_r^{ref}(\lambda, \vartheta_r, \phi_r)$ reflected by the reference plate into the direction (ϑ_r, ϕ_r) is:

$$\Phi_r^{ref}(\lambda, \hat{\vartheta}_r, \hat{\phi}_r) = A_0 S(\lambda) L_0(\lambda) \rho_{BRDF}^{ref}(\lambda, \hat{\vartheta}_0, \hat{\phi}_0, \hat{\vartheta}_r, \hat{\phi}_r) \cos \hat{\vartheta}_0 \Delta \hat{\Omega}_r \quad (5)$$

with $\Delta \hat{\Omega}_r = \int_{\Omega_v} \cos \vartheta_v d\Omega_v$. For a measurement executed with a generic target we obtain a similar expression for the reflected flux. The target-to-reference ratio fluxes $\rho_{acq}(\lambda, \vartheta_0, \phi_0, \vartheta_r, \phi_r)$ obeys the following expression:

$$\rho_{acq}(\lambda, \vartheta_0, \phi_0, \vartheta_r, \phi_r) = \frac{\rho_0^{tar}(\lambda) h^{tar}(\vartheta_0, \phi_0, \vartheta_r, \phi_r) \cos \vartheta_0 \Delta \Omega_r}{\rho_0^{ref}(\lambda) h^{ref}(\hat{\vartheta}_0, \hat{\phi}_0, \hat{\vartheta}_r, \hat{\phi}_r) \cos \hat{\vartheta}_0 \Delta \hat{\Omega}_r} \quad (6)$$

During our measurements the white reference plate always was observed at a fixed geometry, and its outcome was employed to normalize any target measurement as stated in Eq.6. We point out that as an effect of ratio the instrument's sensitivity $S(\lambda)$ is cancelled from the retrieved signal $\rho_{acq}(\lambda, \vartheta_0, \phi_0, \vartheta_r, \phi_r)$ from which we can deduce the complete target BRDF as explained in the following. Under the discussed experimental set-up the goniometric head allows a relative measurement of the bi-directional reflectance function. The measured reflectance spectrum $\rho_{acq}(\lambda, \vartheta_0, \phi_0, \vartheta_r, \phi_r)$ can be expressed as the product of a constant α , which takes into account the directional properties of the reference standard, and the target $\rho_{BRDF}(\lambda, \vartheta_0, \phi_0, \vartheta_r, \phi_r)$ bi-directional reflectance distribution function.

$$\rho_{acq}(\lambda, \vartheta_0, \phi_0, \vartheta_r, \phi_r) = \alpha \rho_0^{tar}(\lambda) h^{tar}(\vartheta_0, \phi_0, \vartheta_r, \phi_r) \cos \vartheta_0 \quad (7)$$

In order to determine the unknown coefficient α we have executed a target measurement of directional-hemispherical reflectance $\rho_{hem}^{tar}(\lambda, \vartheta_0, \phi_0, 2\pi_r)$ with a Perkin Elmer Lambda 19 double-monochromator, which operates from ultraviolet (UV) to short-wave infrared (SWIR), using a deuterium lamp (UV range) and a tungsten-halogen lamp (VIS-NIR and SWIR ranges) as radiation sources. Then, integrating numerically Eq.7

for a complete set of angular measurements we obtain an experimental estimate of the target directional-hemispherical reflectance $\rho_{\text{exp}}^{\text{tar}}(\lambda, \theta_0, \phi_0, 2\pi_r)$. The ratio between this two estimates is related to the constant α .

4. PRELIMINARY RESULTS

A first set of measurements have been performed using a sample of sand (PBU4) with grain size of 0.4-0.6 mm. Measurements were performed placing both the illuminating and viewing fiber on the same azimuthal plane and varying the viewing angle after having fixed the source zenith angle. In Figures 3-6 reflectance contour plots versus wavelengths and viewing zenith angles are reported for an illumination zenith angle of 0°, 15°, 30°, and 45°.

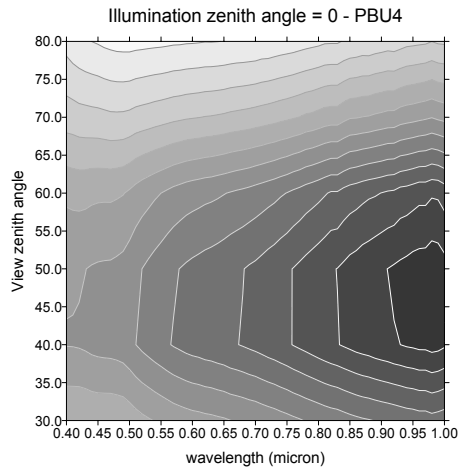


Figure 3. Reflectance contour plots for PBU4 sand versus viewing zenith angles and wavelengths for illumination zenith angle $\theta_i = 0^\circ$ degree.

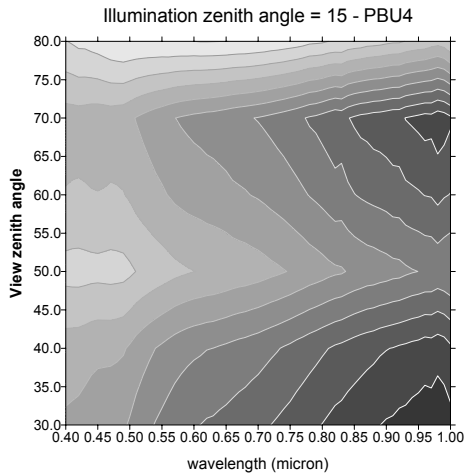


Figure 4. Reflectance contour plots for PBU4 sand versus viewing zenith angles and wavelengths for illumination zenith angle $\theta_i = 15^\circ$ degree.

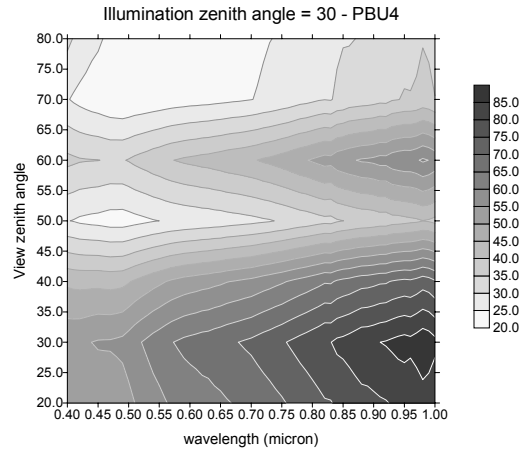


Figure 5. Reflectance contour plots for PBU4 sand versus viewing zenith angles and wavelengths for illumination zenith angle $\theta_i = 30^\circ$ degree.

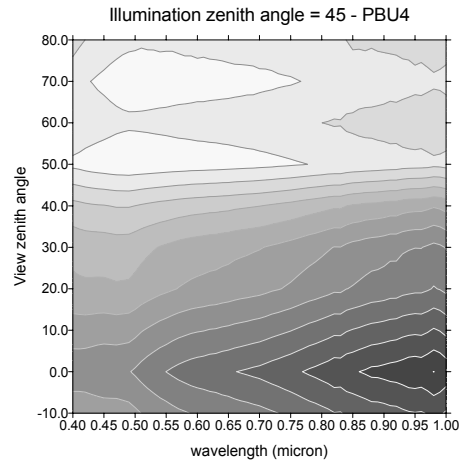


Figure 6. Reflectance contour plots for PBU4 sand versus viewing zenith angles and wavelengths for illumination zenith angle $\theta_i = 45^\circ$ degree.

Figure 7 and Figure 8 show bi-directional reflectance versus illumination and viewing zenith angles for two wavelengths (0.5 μm and 0.8 μm).

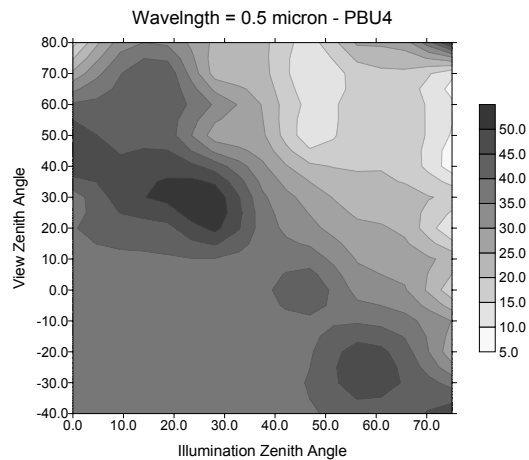


Figure 7. Contour plot of directional reflectance versus illumination and viewing angles at 0.5 μm for PBU4 sand.

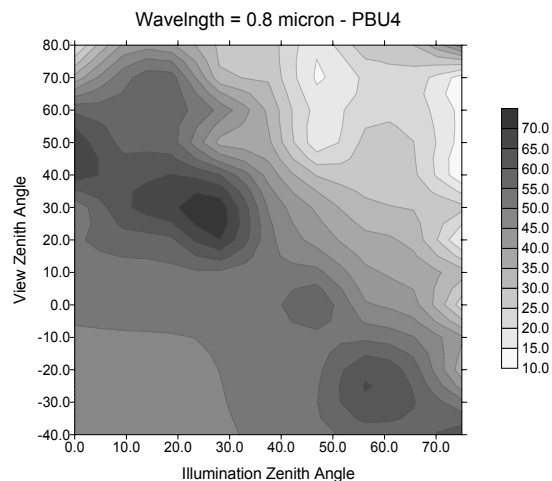


Figure 8. Contour plot of directional reflectance versus illumination and viewing angles at 0.8 μm for PBU4 sand.

6. CONCLUDING REMARKS

In this paper a set of laboratory multiangular observations have been presented in order to retrieve BRDF of sand. A detailed description of the developed instrument has been given with particular reference to the calibration procedure to take account for the angular behaviour of the white standard employed as reference measurement.

The need to improve the modelling of BRDF of natural surface has arisen from the analysis of preliminary results, together with the possibility to consider a not collimated radiation source and to extend the range of viewing zenith angles.

Future investigations will regard the effects of atmosphere on the retrieval of reflectance from multiangle remote sensing data.

7. REFERENCES

Reichman, J., 1973. Determination of Absorption and Scattering Coefficients for Nonhomogeneous Media. 1: Theory, Applied Optics, Vol. 12, No. 8, pp. 1811 – 1815.

Chappelle, E., W., Kim, M., S., McMurtrey III, J., E., 1992. Ratio Analysis of Reflectance Spectra (RARS): An Algorithm for Remote Sensing Estimation of the Concentration of Chlorophyll A, Chlorophyll B, and Carotenoids in Soybean Leaves, Remote Sensing of Environment, 39, pp. 239 – 247.

Pinty, B., Ramond, D., 1986. A simple bi-directional reflectance model for terrestrial surfaces, Journal of Geophysical Research, Vol. 91, No. D7, pp. 7803 – 7808.

Barducci, A., Pippi, I., 1994. Atmospheric Effects Evaluation for the AVIRIS Image-Data Correction or Retrieval, Proceeding of SPIE – Recent Advances in Remote Sensing and Hyperspectral Remote Sensing, EUROPTO Series, 2318, pp. 10 – 16.

Qiu, J., 2001. An improved model of surface BRDF-atmospheric coupled radiation, IEEE Transactions on Geoscience and Remote Sensing, Vol. 39, n. 1, pp. 181 – 187.

Martonchik, J., V., Davide, J., D., Pinty, B., Verstraete, M., M., Myneni, R., B., Knyazikhin, Y., and Gordon, R., 1998. Determination of Land and Ocean Reflective, Radiative, and Biophysical Properties Using Multiangle Imaging, IEEE

Transactions on Geoscience and Remote Sensing, Vol. 36, No. 4, pp. 1266 – 1281.

Miesch, C., X., Briottet, and Kerr, Y., 2002. Bidirectional reflectance of a rough anisotropic surface, International Journal of Remote Sensing, Vol. 23, No. 15, pp. 3107 – 3114.

Sandmeier, S., Muller, C., Hosgood, B., Andreoli, G., 1998. Sensitivity Analysis and Quality Assessment of Laboratory BRDF data, Remote Sensing of Environment, Vol. 64, pp. 176 – 191.

Sandmeier, S., Itten, I., K., 1999. A field goniometer system (FIGOS) for acquisition of hyperspectral BRDF data, IEEE Transactions on Geoscience and Remote Sensing, Vol. 37, No. 2, pp. 978 – 986.

Deering, D., W., and Leone, P., 1986. A sphere-scanning radiometer for rapid directional measurements of sky and ground radiance, Remote Sensing of Environment, Vol. 19, pp. 1 – 24.

Voss, K., J., Chapin, A., Monti, M., and Zhang, H., 2000. Instrument to measure the bi-directional reflectance distribution function of surfaces, Applied Optics, Vol. 39, No. 33, pp. 6197 – 6206.

Diner, D., J., Beckert, J., C., Reilly, T., H., Bruegge, C., J., Conel, J., E., Kahn, R., A., Martonchik, J., V., Ackerman, T., P., Davies, R., W., Gerstl, S., A., Gordon, H., R., Muller, J-P., Myneni, R., B., Sellers, P., J., Pinty, B., and Verstraete, M., M., 1998. Multi-angle Imaging Spectroradiometer (MISR) instrument description and experiment overview, IEEE Transactions on Geoscience and Remote Sensing, Vol. 36, pp. 1072 – 1087.

Cutter, M., A., Johns, L., S., Lobb, D., R., Williams, T., L., Settle, J., J., 2003. Flight Experience of the Compact High Resolution Imaging Spectrometer (CHRIS), Proceeding of SPIE Conference 5159 Imaging Spectrometry IX, August 2003, San Diego, California, USA.

Nicodemus, F., E., Richmond, J., C., Hsia, J., J., Ginsberg, I., W., and Limperis, T., 1977. Geometrical considerations and nomenclature for reflectance, Technical Report NBS MN-160, National Bureau of Standards.